Neuron
Report

Prestin-Based Outer Hair Cell Motility Is Necessary for Mammalian Cochlear Amplification

Peter Dallos,[1,4,*] Xudong Wu,[2] Mary Ann Cheatham,[4] Jiangang Gao,[2] Jing Zheng,[4] Charles T. Anderson,[4] Shuping Jia,[3] Xiang Wang,[3] Wendy H.Y. Cheng,[2] Soma Sengupta,[4] David Z.Z. He,[3,5] and Jian Zuo[2,5,*]
[1]Department of Neurobiology and Physiology, Northwestern University, Evanston, IL 60208, USA
[2]Department of Developmental Neurobiology, St. Jude Children's Research Hospital, Memphis, TN 38105, USA
[3]Department of Biomedical Sciences, Creighton University, Omaha, NE 68178, USA
[4]Department of Communication Sciences and Disorders, The Hugh Knowles Center, Northwestern University, Evanston, IL 60208, USA
[5]These authors contributed equally to this work.
*Correspondence: p-dallos@northwestern.edu (P.D.), jian.zuo@stjude.org (J.Z.)
DOI 10.1016/j.neuron.2008.02.028

SUMMARY

It is a central tenet of cochlear neurobiology that mammalian ears rely on a local, mechanical amplification process for their high sensitivity and sharp frequency selectivity. While it is generally agreed that outer hair cells provide the amplification, two mechanisms have been proposed: stereociliary motility and somatic motility. The latter is driven by the motor protein prestin. Electrophysiological phenotyping of a prestin knockout mouse intimated that somatic motility is the amplifier. However, outer hair cells of knockout mice have significantly altered mechanical properties, making this mouse model unsatisfactory. Here, we study a mouse model without alteration to outer hair cell and organ of Corti mechanics or to mechanoelectric transduction, but with diminished prestin function. These animals have knockout-like behavior, demonstrating that prestin-based electromotility is required for cochlear amplification.

INTRODUCTION

In the mammalian cochlea, it is assumed that outer hair cells (OHC) are the amplifiers and that inner hair cells (IHC) are passive detectors of the amplified vibratory signal (e.g., Dallos, 1992). This assumption has a long history that began with chemical ablation of OHCs and demonstration of significant effects on hearing threshold (Ryan and Dallos, 1975) and frequency selectivity (Dallos and Harris, 1978). Crawford and Fettiplace (1985) demonstrated voltage-dependent movement of the stereocilia in the turtle cochlea, and Brownell et al. (1985) discovered somatic motility of mammalian OHCs, establishing the groundwork for two competing theories of cochlear amplification. Both reports engendered follow-up, with somatic motility enjoying broader support as the principal mechanism of amplification in mammals. However, two recent publications (Chan and Hudspeth, 2005; Kennedy et al., 2005), and their numerous antecedents, appear to support the ciliary mechanism (Hudspeth, 1997).

The need for amplification is sought in the highly damped nature of the cochlear partition, which, without some boost, would not permit sharply tuned, sensitive operation (Gold, 1948). Consequently, a process is required to counteract the damping by injecting mechanical energy on a cycle-by-cycle basis (Neely and Kim, 1983; DeBoer, 1986). Because tuning curves obtained from single auditory nerve fibers are similar to those recorded at the basilar membrane (Narayan et al., 1998), this amplifier process must influence all elements of the coupled cochlear mechanical system. Thus, it is not sufficient for the amplifier to operate on the mechanoelectric transducer (MET) channels alone, i.e., its operation must be reflected in the vibration of all components, including the basilar membrane. This requirement dictates that there be an adequate mechanical impedance match between the amplifier and its load. If the stiffness of a constituent mechanical element (such as the OHC) changes, so does its impedance, and, consequently, a match is no longer obtained, resulting in decreased amplification.

OHC somatic electromotility is powered by the novel motor protein prestin (SLC26A5: Zheng et al., 2000). OHCs isolated from the prestin-KO mouse were not motile, and the electrophysiological phenotype was consistent with the lack of amplification (Liberman et al., 2002). Despite normal appearance of hair bundles (Wu et al., 2004) and expression of candidate ciliary-motor proteins (Liberman et al., 2002), there was insufficient evidence as to the integrity of the forward transduction mechanism. Subsequently, forward transduction was shown to be normal in the KO mouse model, supporting the dominant role of somatic motility in amplification (Cheatham et al., 2004; Jia and He, 2005). Although this body of work was suggestive, confounding features indicated a need for caution, including the shorter OHC length (~60% of normal; Liberman et al., 2002; Cheatham et al., 2004, 2007), intimating the possibility of abnormal cochlear micromechanics. Given the importance to amplification of impedance matching of the amplifier to its cochlear load, a significant change in the mechanical load could simulate the no-amplification phenotype. As previous studies of the KO did not examine mechanical integrity, the behavior of the prestin KO mouse cannot be unequivocally assigned to a lack of amplification via somatic motility. As a result, a different model is needed.

RESULTS

Creation and Properties of the 499 KI Mouse

To further examine the role of prestin in cochlear amplification, we created a prestin knockin (KI) mouse in which 2 residues

were replaced (V499G/Y501H; Figure 1A; for simplicity, the altered molecule is referred to as "499" and the V499G/Y501H knockin mouse as "KI") near the presumed junction between the last transmembrane domain and the intracellular C terminus. Choice of these substitutions was based on earlier studies (Zheng et al., 2005), showing that 499 mutant prestin is targeted to the plasma membrane but displays significantly diminished functional characteristics, i.e., nonlinear capacitance (NLC). NLC reflects electromotility-related charge displacement in OHCs and is commonly used to assess motor function (Ashmore, 1990; Santos-Sacchi, 1991).

Although 499 homozygous mice suffer progressive OHC loss in the basal cochlear turn, individual OHCs have normal lengths (WT: 15.4 ± 0.62 mm; 499: 15.1 ± 1.1 mm; n = 30 each, measured ~500 μm from the base of the cochlea; Student's t test, p = 0.15). We also measured OHC somatic stiffness in cells derived from KI, WT, and KO mice. As shown in Figure 1B, a calibrated glass fiber is positioned against the cuticular plate of an OHC with ~80% of its length extruded from a microchamber. Measurements of axial stiffness (Figure 1C) indicate that OHCs from WT and 499 mice are equally stiff. We tested this similarity with the "two regression lines" test (Tsutakawa and Hewett, 1978). Regressions representing the two populations (KI and WT) are not statistically different (p = 0.27). In contrast, regressions of both WT and KI are significantly different from that of the KO, with the somatic stiffness of OHCs derived from KO mice between one-fourth and one-third that of WT controls. These findings yield two important conclusions. First, inasmuch as OHCs of KI mice are mechanically similar to those of WT, the KI is appropriate for assessing prestin-based amplifier function. Second, the KO is not a usable model to test the importance of prestin-based electromotility in cochlear amplification.

Because mutations in prestin often cause protein misfolding and interfere with proper membrane targeting (Zheng et al., 2005; He et al., 2006), we compared wild-type and mutant prestin protein expression patterns in cochleae derived from WT and KI mice using immunofluorescence. For each genotype, one cochlea was treated with Triton X-100 to permeabilize the plasma membrane. As shown in Figure 2A, cochleae derived from WT and KI mice have similar prestin staining patterns (demonstrated with anti-C-mPres). Immunofluorescence is only observed with Triton X-100 pretreatment, suggesting that the C terminus of the 499 mutant protein is located inside cells as with the WT. The typical "ring" staining pattern of OHCs observed in organ of Corti samples suggests that prestin and mutant prestin are restricted to the lateral membrane of OHCs. Similar results were also found with anti-N-mPres. In addition, we investigated the oligomeric status (Zheng et al., 2006) of mutant prestin. Similar to WT, 499 prestin forms monomers and dimers, and the dimer bands disappear after pretreatment with the reducing reagent ethanedithiol (Figure 2B). There is no statistical difference between WT and 499-prestin in the amounts of monomer and dimer, or their ratio (Figure 2C). In combination, these results suggest that 499 KI mice possess normal cochlear/OHC structural and mechanical properties.

In Vitro Experiments

As shown in Figures 3A and 3B, OHCs derived from 499 animals express significantly reduced nonlinear capacitance and electromotility compared to WT littermates. It also appears that the mutation induces a large positive-direction shift in both NLC and motility, with a concomitant reduction in response magnitude around the OHC resting potential. While the saturated motile and NLC responses cannot be reached in the 499 OHCs (due to membrane breakdown at very large depolarized membrane potentials), they appear to be small. This behavior recapitulates that seen with severe reduction of intracellular chloride (Rybalchenko and Santos-Sacchi, 2003). More importantly, at the putative in vivo membrane potential of −70 mV (Dallos, 1985; Russell and Sellick, 1983), the slope of the average motility function changes from 7.10 nm/mV (WT) to 0.53 nm/mV (499 KI). Thus, the gain of amplification based on somatic motility is on average 7.5% of normal. From the model proposed by Patuzzi (1996), the expected threshold shift based on the 7.5% gain is ~54.5 dB, which is indistinguishable from that exhibited by KO animals (Cheatham et al., 2004).

In order to assess the contribution of prestin-based somatic electromotility to cochlear amplification, it is essential to

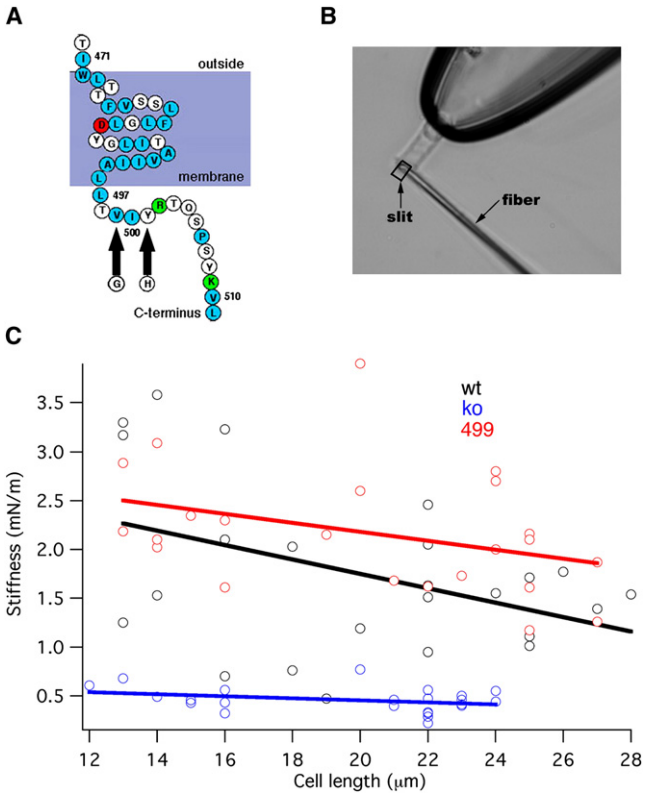

Figure 1. The 499/501 Mutation and Hair Cell Stiffness

(A) Partial amino acid sequence of the predicted topology of prestin showing the last putative membrane-spanning helix and partial C terminus. Arrows indicate the 499/501 mutation.

(B) KO mouse OHC held by a microchamber, along with a driven fiber positioned against the cell's ciliated pole for stiffness determination. The joint displacement of fiber and cell is monitored by a photodiode through a rectangular slit.

(C) Plots of OHC somatic stiffness versus cell length. Wild-type (black, n = 22), prestin KO (blue, n = 21), and 499 KI (red, n = 23); this color scheme will be followed in all subsequent plots. Lines are linear regression fits to the data.

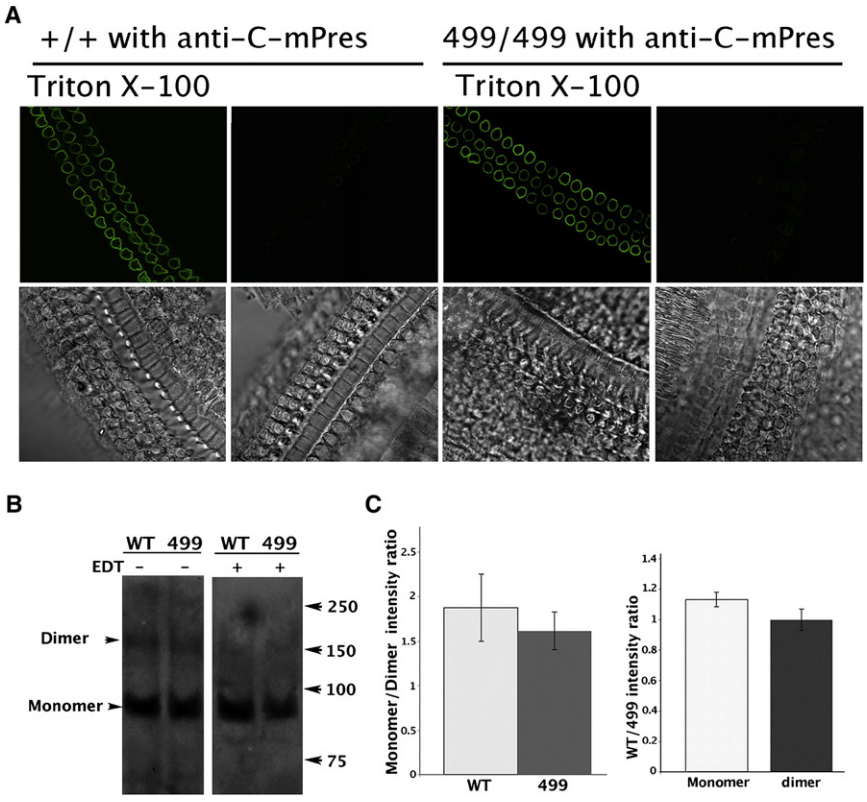

Figure 2. Membrane Targeting and Oligomeric Status

(A) Plasma membrane targeting of prestin in OHCs of WT and 499 KI mice. Whole-mount preparations of apical cochlear turns of WT and 499 mice at P25. Immunofluorescent images derived from WT (first two images) and 499 homozygous mice (second two images) stained with anti-C-mPres. First and third images: treatment with Triton X-100, second and fourth images: no treatment.

(B) Prestin's oligomeric status in WT and 499 cochleae examined by NEXT-PAGE/Western blot. EDT, ethanedithiol.

(C) Intensities of monomer and dimer bands compared between WT and 499 cochleae. No statistical difference between the amounts of monomer (t test, $p = 0.11$), dimer ($p = 0.99$), or their ratio ($p = 0.59$; $n = 3$) is seen.

demonstrate that MET channel function, the basis of ciliary motility, is intact. Accordingly, we demonstrate that MET currents are wild-type like, strongly suggesting that forward transduction is unaltered in these animals. In Figure 3C, two individual examples are shown for current traces measured in response to increasing sinusoidal displacements of the basilar membrane. Average (±SD) change in transducer current is depicted in Figure 3D ($n = 5$ each). The difference between the average behaviors was tested with ANOVA and found to be insignificant ($F = 1.62$, $p = 0.24$). Finally, Figure 3E demonstrates that fast adaptation, presumably intimately tied to stereociliary amplification (e.g., LeMasurier and Gillespie, 2005), is also indistinguishable from that seen in wild-type mice. For example, low-level average fast adaptation time constants are 0.120 ± 0.011 ms for WT ($n = 5$) and 0.120 ± 0.006 ms for 499 ($n = 5$) (t test: $p = 0.62$). All of the in vitro data shown thus far indicate that the 499 KI mice provide an ideal model for testing the hypothesis that prestin is required for cochlear amplification.

In Vivo Experiments

Recordings of various indices of cochlear performance are shown in Figure 4. Included are compound action potential (CAP) threshold functions (Dallos et al., 1978; Johnstone et al., 1979) and CAP simultaneous masking tuning curves (Dallos and Cheatham, 1976). The first measure provides a description of hearing sensitivity, i.e., the CAP threshold curves reflect the animals' audiogram. The second index, CAP masking tuning curve, provides a measure of the threshold characteristics of a small group of auditory nerve fibers with similar characteristic frequencies, i.e., they provide an indication of frequency selectivity at the "output" of the cochlea. Figure 4A shows CAP thresholds for 499 and corresponding WT mice (average ± SD, $n = 7$ each). CAP threshold is defined as the sound pressure level at the eardrum required to produce a criterion magnitude CAP at a given frequency. The 499 animals show a large threshold shift compared to WT. As seen previously in KOs (Cheatham et al., 2004), mice lacking functional prestin exhibit a large change in sensitivity. In Figure 4B, the average difference between individual 499 threshold curves and the average WT threshold curve is given. Included for comparison is the average CAP threshold difference for prestin KO mice ($n = 8$) and their WT controls ($n = 10$). We note that the threshold shift changes from ~30 dB at low frequencies to ~55 dB at 27 kHz. The decrease at the highest frequencies is due to age-related hair cell loss, which produces high-frequency threshold shift even in WT animals (Figure 4A; shaded region). The apparent reversal at the lowest frequencies, where thresholds are determined by the tail-sensitivities of high-frequency fibers, is unexplained. An ANOVA to test for differences between 499 and KO resulted in an F ratio of 0.29 and $p = 0.59$. It is apparent that 499 KI and prestin KO threshold shifts are not statistically different. In addition, click auditory brainstem responses corroborate the CAP measurements (data not shown). Finally, in Figure 4C, CAP average (±SD) masking tuning curves are shown for 499 KI ($n = 7$) and WT ($n = 5$) mice. As in KO animals (Cheatham et al., 2004, 2007), tuning is absent in the 499 mice.

DISCUSSION

Outer hair cell mediated mechanical amplification is a signal feature of the mammalian cochlea (e.g., Dallos, 1992). However, in spite of extensive research, there is no general agreement as to the mechanism of amplification. In theory, either ciliary or

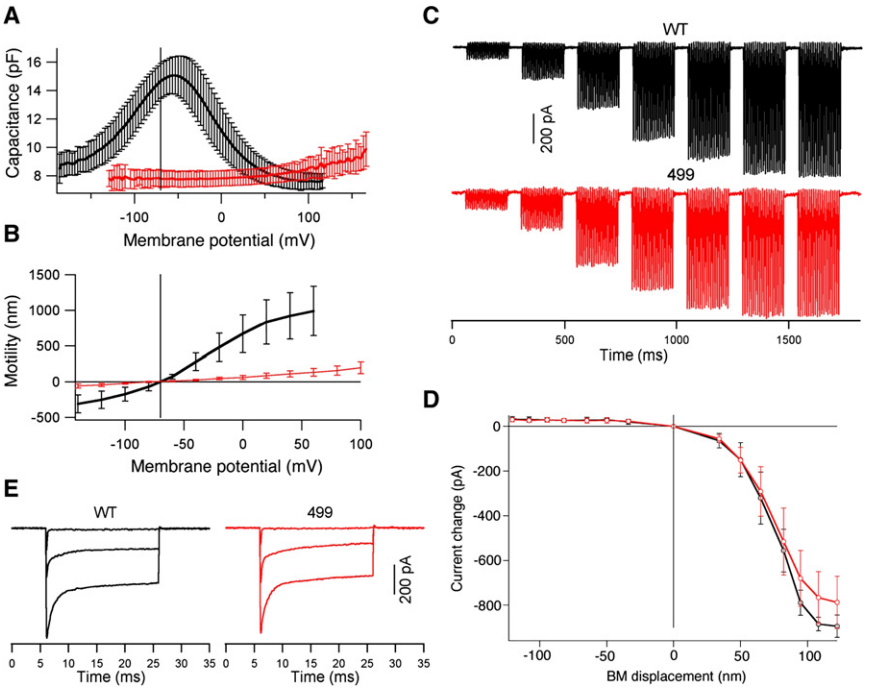

Figure 3. In Vitro Measurements of Hair Cell Function

(A) Average NLC (±SD) for WT and 499 OHCs (499, n = 8; WT, n = 11).

(B) Average motility (cell-length change) ± SD (WT, n = 11; 499, n = 9). Cell contraction is plotted up. Linear capacitance values, measured as the asymptotes of the NLC curves at large positive (WT) and negative (499) membrane potential are similar. (Clin ± SD for WT: 7.8 ± 0.9 pF and 499: 7.80 ± 0.66 pF; t test: p = 0.72).

(C) Representative transducer currents in response to 100 Hz sinusoidal displacements of the basilar membrane from WT and 499 OHCs in the hemicochlea. BM displacement varied between approximately ±120 nm in equal steps (inward current is down, holding potential −70 mV).

(D) Average (±SD, n = 5 WT; n = 5 KI) change in transducer current magnitude in response to sinusoidal displacements of the BM.

(E) Representative transducer currents in response to 20 ms DC displacement of the TM toward scala tympani for a WT and 499 OHC.

somatic motility mechanisms could provide amplification in the mammal; which one does and in what manner is a central question of cochlear neurobiology.

If cochlear amplification is explained by *either* ciliary *or* somatic processes, and one wishes to select between the two, the present results rule out ciliary amplification. Accordingly, prestin KI mice display their characteristic phenotype because they lack an amplifier and not because the micromechanical load on the ciliary amplifier is altered. Support for this statement comes from results reported here showing normal OHC length and stiffness, as well as normal MET function. Thus, one may surmise that, in spite of mechanical changes in OHCs lacking prestin, the KO mouse lacks sensitivity and frequency selectivity because amplification is absent and not because the mechanical properties of its OHCs are altered. Our recent study, using a different prestin KI model, is in line with this conclusion (Gao et al., 2007).

Alternatively, these two putative amplifier processes might cooperate (e.g., Fettiplace, 2006). In its most advanced form, this model envisions ciliary motility to be the amplifier, with somatic motility adjusting its operating point. The adjustment presumably minimizes the DC component of the OHC receptor potential by shifting the operating point of the mechanoelectric transducer via somatic-motility feedback. Supporting this schema is the observation that intracellular receptor potentials from OHCs in the high-frequency region of the cochlea reveal symmetrical AC responses with virtually no DC component up to high sound levels (Russell and Sellick, 1983; Cody and Russell, 1987). One problem with this argument is that using an alternative approach to intracellular recording from OHCs in vivo, well-developed DC responses are measured from the entire apical half of the cochlea, including regions where cochlear amplification is clearly operative (Dallos, 1985; Cheatham and Dallos, 1993). Hence, the existence or lack of a DC receptor potential throughout the cochlea is not conclusively established. Another potential problem with this notion is the universal presence of adaptation in all hair cell systems studied (e.g., Eatock, 2000). Functionally, adaptation of the MET apparatus is a nonlinear high-pass filter, particularly effective at low input levels where amplification is maximal. As a high-pass filter, adaptation reduces the effectiveness of DC feedback from somatic motility to the MET transducer, i.e., the putative ciliary amplifier.

Assuming separate functions for the two processes, we ask what role might be played by feedback mechanisms associated with the MET channels. MET channels function as amplifiers in hair cell systems of lower vertebrates (Hudspeth, 1997; Manley, 2001). It has been demonstrated that ciliary processes may also tune the transducer current to cell-specific frequencies (Martin and Hudspeth, 1999). In fact, in all models of ciliary feedback, tuning and amplification are intimately associated. It is possible that in mammals the reciprocal behavior of MET channels is principally represented by frequency tuning of the OHC transducer current, with the amplificatory behavior effectively squelched by the significant mechanical load. The latter is manifest by the need to displace the basilar membrane-tectorial membrane complex by forces generated in the MET channels. This putative inability, however, should not preclude tuning. One can envision a scheme whereby a division of labor is established between the ciliary (MET) process and prestin. The former tunes the transducer current so that in any hair cell only a relatively narrow, tonotopically arranged frequency band produces AC voltage gradients, thereby activating prestin motors, which are fully responsible for amplification. Although this dichotomy between tuning and amplification has been intimated before (Robles and Ruggero, 2001), its clearest expression is given by Ricci (2003): "It is likely that OHC motility provides the mechanical

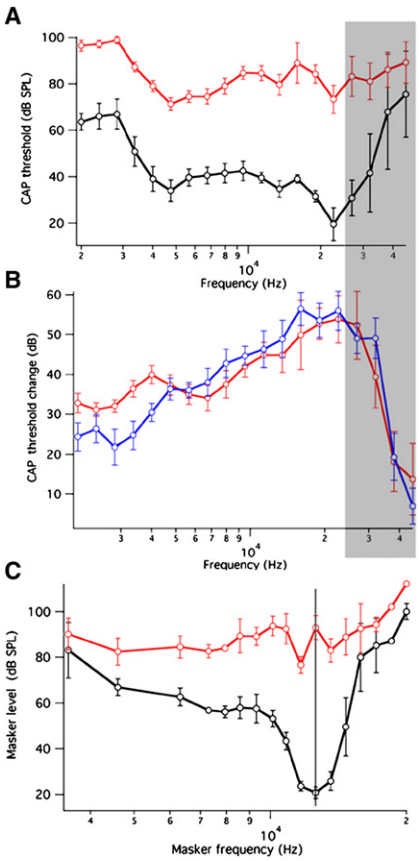

Figure 4. CAP Data Obtained from a Round-Window Electrode

(A) Average (±SD, n = 6 WT; n = 7 KI) CAP thresholds (sound pressure level required to measure10 μV CAP) as a function of stimulus frequency for 499 KI and WT mice.

(B) Average differences (±SD) between individual 499 KI thresholds and the corresponding average WT threshold (red). Average differences (±SD) between individual prestin KO thresholds and the corresponding average WT threshold (blue). The KO mice were described in Cheatham et al. (2007). Shaded region approximately corresponds to extent of age-related hair cell loss.

(C) Average (±SD) CAP masking tuning curves for 499 KI (n = 7) and WT mice (n = 5). Probe tone frequency: 12 kHz. Inasmuch as our tuning-curve collection platform uses slightly different masker frequencies for each tuning curve, an average frequency scale was created. As a consequence, the average WT tuning curve appears to be more shallowly tuned than those published previously (Dallos and Cheatham, 1976; Cheatham et al., 2004, 2007).

positive feedback but that this feedback is tuned by some other component, namely the sensory hair bundle." Recent demonstrations that voltage-induced bundle motion is, either fully (Jia and He, 2005) or at least in significant part (Kennedy et al., 2006), due to somatic motility support this possibility. Longitudinally graded OHC transducer currents and fast adaptation time constants also support the possibility of a location-specific cilia-based tuning mechanism (He et al., 2004; Ricci et al., 2005). It has also been shown that the reduction in driving force to somatic motility at high frequencies, due to attenuation of the AC receptor potential by filtering at the OHC's basolateral membrane, can be overcome in various ways (see Dallos et al., 2006). Finally, prestin's dominant role in amplification is supported by recent in vivo experiments (Santos-Sacchi et al., 2006).

If prestin developed in order to produce a DC adjustment to the operating point of the MET channel, as theories of cooperativity suggest, one might question the use of a novel protein for this purpose. What sets prestin apart from other biological motors is its direct voltage-to-displacement conversion process and its speed. The protein is capable of producing force at rates exceeding 70 kHz (Frank et al., 1999). Hence, one asks what might be the evolutionary advantage of converting a sulfate transporter into a high-speed motor and then using it only at DC when conventional enzymatic motors could have fulfilled this role. It appears to us that assigning amplification to prestin and perhaps prefiltering to the MET channel is a reasonable means of achieving OHC function at any stimulus frequency in mammals. Nevertheless, neither the prestin KO nor any of the KI models studied so far is capable of discriminating between models in which prestin is the sole amplifier and in which prestin-based DC motility adjusts the MET operating point. This is due to the simple fact that as the "gain" of prestin is turned down, both amplification and operating point adjustment are reduced. What the electrophysiological results from prestin mutant animals unequivocally show is that the normal molecule is essential for cochlear amplification. Without demonstrating normal mechanical properties and intact MET function, as done in the present work, this conclusion could not have been reached.

EXPERIMENTAL PROCEDURES

Prestin 499 KI Mice

See the Supplemental Data available online.

Immunocytochemistry

Animals were perfused intracardially with heparinized PBS followed by 4% formaldehyde in PBS. After ~2 hr postfixation at RT, cochleae were dissected, with one receiving 0.2% Triton X-100/PBS. Ten percent normal goat serum was used to block nonspecific binding. Tissue samples were incubated with anti-C-mPres or anti-N-mPres antibodies. Samples were washed with PBS, incubated with 2° antibodies, mounted on glass slides with Fluoromount-G (Southern Biotechnology Associates, Inc., Birmingham, AL), and observed with a Leica confocal system with a standard configuration DMRXE7 microscope.

NEXT-PAGE/Western Blotting

A pair of cochleae from WT and 499/499 mice was collected in 50 ml CelLytic Mammalian Tissue Lysis/Extraction Reagent (Sigma C3228) supplemented with 100 μg/ml phenylmethylsulfonylfuoride, 1:50 protease inhibitor cocktail (Sigma P8340), 10 U/ml DNase. After homogenization, low-speed centrifugation (3000 × g for 10 min) was applied to separate nuclei, unlysed cells, and bone structures. Half of the cell lysates were mixed with 2X LDS Laemmli sample buffer alone; the other with 2X LDS Laemmli sample buffer containing 200 mM of the reducing agent ethanedithiol (EDT). Samples were loaded on a 5% NEXT gel (AMRESCO, Solon, OH). After separation, gel proteins were electrotransferred onto a nitrocellulose membrane (Millipore), blocked with 5% nonfat dry milk and reacted with primary (anti-C-mPres) and secondary antibodies (donkey anti-rabbit IgG-HRP). Immunoreactive bands were visualized with the ECL western blotting detection system (Pharmacia). The integrated intensity of prestin bands was measured in arbitrary units using Kodak ID Image Analysis software as described before (Cheatham et al., 2005).

Measurement of Nonlinear Capacitance

OHCs were isolated via enzymatic digestion and gentle trituation and bathed in an extracellular solution containing (in mM) 120 NaCl, 20 TEA-Cl, 2 $CoCl_2$,

2 $MgCl_2$, 10 HEPES, and 5 glucose, pH 7.3. The internal solution contained (in mM) 140 CsCl, 2 $MgCl_2$, 10 EGTA, and 10 HEPES, pH 7.3. Whole-cell voltage-clamp recording was at RT (Axopatch 200B, Molecular Devices Corp. Sunnyvale, CA). A two-sine voltage stimulus protocol (10 mV peak at both 390.6 and 781.2 Hz) with subsequent fast Fourier transform-based admittance analysis was used to measure membrane capacitance (0 mV holding potential). Capacitive currents were sampled at 20 kHz and low-pass filtered at 5 kHz. Series resistance was compensated off-line. Data were acquired using jClamp (version 11.1, Scisoft, New Haven, CT).

Measurement of Somatic Motility

Solitary OHCs were bathed in extracellular solution (described above). OHCs were voltage clamped, and motility was measured with an electro-optical technique, with the cell's ciliated pole imaged onto a photodiode through a rectangular slit. The photocurrent was proportional to the displacement of the cell's image in the slit. Movements were calibrated by moving the slit a known distance (1 μm) with a piezoelectric driver.

Measurement of OHC Axial Stiffness

Healthy OHCs were drawn into a microchamber (Dallos et al., 1991) with ~80% of their length extruded. Glass fibers were pulled from 1.5 mm glass tubing using a microforge (Narashige, East Meadow, NY). The tapered tip of a fiber was usually 4–5 mm in length and 2–3 μm in diameter. Fiber stiffness ranged between 1.2 and 3.3 mN/m and was calibrated as in Howard and Ashmore (1986). The glass fiber was attached to a single-axis piezoelectric actuator mounted on a three-axis micromanipulator. The tip of the glass fiber was brought against the cuticular plate of the cell, transverse to the OHC's long axis, so that its lateral motions would compress or relax the cell. Two quantities were measured: "free fiber motion," the displacement of the tip of the fiber when driven by the bimorph actuator (vibrating at 100 Hz) but not loaded by the cell; and "loaded fiber motion," the joint displacement of the junction between cell and fiber after the fiber was loaded onto the cell. Axial stiffness was computed from the amplitude difference between loaded and unloaded responses (He and Dallos, 1999). Inasmuch as stiffness determines the low-frequency behavior of the cell's mechanical impedance, it is best measured at low frequencies; hence, the choice of 100 Hz. The mean ages of animals used were 28.7 ± 4.2 days (WT), 27.6 ± 3.4 days (KO), and 26.0 ± 2.7 days (499 KI).

Recording Mechanotransducer Currents in the Mouse Hemicochlea

Hemicochleae were prepared from young mice and mounted on an upright Leica microscope with water-immersion objectives (Keiler and Richter, 2001). The L-15 bathing medium contained (in mM) 136 NaCl, 5.8 NaH_2PO_4, 5.4 KCl, 1.4 $CaCl_2$, 0.9 $MgCl_2$, 0.4 $MgSO_4$, 10 HEPES-NaOH, at pH 7.4 and 300 mosm L^{-1}. The internal solution contained (in mM) 140 CsCl, 0.1 $CaCl_2$, 3.5 $MgCl_2$, 2.5 MgATP, 5 EGTA-KOH, 5 HEPES-KOH, at pH 7.4 and 300 mosm L^{-1}. Pipette resistances were 3–4 MΩ. Recordings were made in whole-cell voltage-clamp with an Axopatch 200B patch-clamp amplifier (Molecular Devices, Sunnyvale, CA). Series resistance was 8–12 MΩ compensated to ~70%. Procedures for measuring MET currents are described elsewhere (Jia et al., 2007). In brief, a thin glass fiber with a tip diameter of 20 mm and a 40 mm spherule at its distal end was used as a paddle to vibrate the basilar membrane (BM). The paddle was mounted on a piezoelectric actuator (Burleigh Driver/Amplifier, PZ-150M), which was mounted on another 3-D Narashige micromanipulator (MHW-3). It was positioned below the midpoint of the pectinate zone, such that paddle vibrations were coupled to the BM through the fluid. Upward motion of the paddle resulted in the BM moving toward the scala vestibuli. 100 Hz sinusoidal voltage bursts with different amplitudes were used. To measure adaptation of the MET currents, the paddle was loaded onto the top surface of the tectorial membrane (TM) underneath Reissner's membrane. Fiber-driven downward step motion of the TM deflected the OHC bundle (Jia et al., 2007). Step-voltage commands generated by a function generator were low-pass filtered at 4.5 kHz before being fed to the piezoelectric actuator. The rise time (between 10% and 90% of steady-state value) of paddle motion after loading onto the TM was 0.08 ms, corresponding to a cut-off frequency of 4.25 kHz. MET currents were sampled at 20 or 50 kHz and filtered at either 1 kHz (for sinusoidal stimulation) or 5 kHz (for adaptation measurement). The current responses are the average of five trials. Data were analyzed using Clampfit (Molecular Devices) and Igor Pro (WaveMetrics, Inc). All procedures were approved by the National Institutes of Health and by Creighton University's Animal Care and Use Committee.

In Vivo Electrophysiology

WT, prestin-KO, and 499 KI mice were anesthetized with sodium pentobarbital (80 mg/kg, IP). Supplemental doses were given throughout to maintain a surgical level of anesthesia. During both surgery and data collection, the head-holder was heated to prevent cooling of the cochlea. All procedures were approved by the National Institutes of Health and by Northwestern University's Animal Care and Use Committee. The mean ages of animals used were 34.7 ± 4.4 days (WT), 33.3 ± 0.95 days (KO), and 30 ± 2.0 days (499 KI). Compound action potential thresholds were acquired with a tracking program, which determined the sound pressure level necessary to generate a 10 μV N1/P1 voltage. In addition, a simultaneous, tone-on-tone masking paradigm (Dallos and Cheatham, 1976) was used to acquire CAP tuning curves. In this procedure, the level of a 12 kHz probe tone, presented alone, was adjusted to generate a response of 25 μV measured between the first negative and subsequent positive peak of the CAP. Masker frequency and level were then varied to produce a 3 dB decrease in the probe response, i.e., to ~18 μV. The masker was presented in alternating phase to minimize the cochlear microphonic. All neural measurements were obtained using a programmable band-pass filter to shape electrical signals between 0.3 and 2.4 kHz and using custom software designed by J.H. Siegel (Visual Basic, Microsoft).

SUPPLEMENTAL DATA

The Supplemental Data for this article can be found online at http://www.neuron.org/cgi/content/full/58/3/333/DC1/.

ACKNOWLEDGMENTS

We thank T. Nicol for advice on statistics and J. Siegel and Y. Yu for technical assistance. R. Edge and K. Miller participated in some immunocytochemistry and K. Naik in some in vivo experiments. This work is supported in part by ALSAC, The Hugh Knowles Center, and by NIH grants DC00089 (to P.D.), DC06471, CA023944, and CA21765, and the Hartwell Foundation (to J. Zuo), DC 004696 (to D.Z.Z.H.), DC006412 (to J. Zheng).

Received: December 11, 2007
Revised: February 14, 2008
Accepted: February 25, 2008
Published: May 7, 2008

REFERENCES

Ashmore, J.F. (1990). Forward and reverse transduction in the mammalian cochlea. Neurosci. Res. Suppl. *12*, S39–S50.

Brownell, W., Bader, C.R., Bertrand, D., and de Ribaupierre, Y. (1985). Evoked mechanical responses of isolated cochlear outer hair cells. Science *227*, 194–196.

Chan, D., and Hudspeth, A.J. (2005). Ca2+ current-driven nonlinear amplification by the mammalian cochlea in vitro. Nat. Neurosci. *8*, 149–155.

Cheatham, M.A., and Dallos, P. (1993). Longitudinal comparisons of IHC AC and DC receptor potentials recorded from the guinea-pig cochlea. Hear. Res. *68*, 107–114.

Cheatham, M.A., Huynh, K.H., Gao, J., Zuo, J., and Dallos, P. (2004). Cochlear function in *Prestin* knockout mice. J. Physiol. *560*, 821–830.

Cheatham, M.A., Zheng, J., Huynh, K.H., Du, G.G., Gao, J., Zuo, J., Navarrete, E., and Dallos, P. (2005). Cochlear function in mice with only one copy of the *prestin* gene. J. Physiol. *569*, 229–241.

Cheatham, M.A., Huynh, K., Zheng, J., Du, G.G., Edge, R.M., Anderson, C.T., Ryan, A.F., Zuo, J., and Dallos, P. (2007). Evaluation of a prestin mouse model derived from the 129S1 strain. Audiol. Neurootol. *12*, 378–390.

Cody, A.R., and Russell, I.J. (1987). The responses of hair cells in the basal turn of the guinea-pig cochlea to tones. J. Physiol. *383*, 551–569.

Crawford, A.C., and Fettiplace, R. (1985). The mechanical properties of ciliary bundles of turtle cochlear hair cells. J. Physiol. *364*, 359–379.

Dallos, P. (1985). Response characteristics of mammalian cochlear hair cells. J. Neurosci. *5*, 1591–1608.

Dallos, P. (1992). The active cochlea. J. Neurosci. *12*, 4575–4585.

Dallos, P., and Cheatham, M.A. (1976). Compound action potential (AP) tuning curves. J. Acoust. Soc. Am. *59*, 591–597.

Dallos, P., and Harris, D.M. (1978). Properties of auditory nerve responses in the absence of outer hair cells. J. Neurophysiol. *41*, 365–383.

Dallos, P., Harris, D.M., Özdamar, Ö., and Ryan, A. (1978). Behavioral, compound action potential, and single unit thresholds: Relationship in normal and abnormal ears. J. Acoust. Soc. Am. *64*, 151–157.

Dallos, P., Evans, B.N., and Hallworth, R. (1991). Nature of the motor element in electrokinetic shape changes of cochlear outer hair cells. Nature *350*, 155–157.

Dallos, P., Zheng, J., and Cheatham, M.A. (2006). Prestin and the cochlear amplifier. J. Physiol. *576*, 37–42.

DeBoer, E. (1986). Mechanics of the cochlea: Modeling efforts. In The Cochlea, P. Dallos, A.N. Popper, and R.R. Fay, eds. (New York: Springer), pp. 258–317.

Eatock, R.A. (2000). Adaptation in hair cells. Annu. Rev. Neurosci. *23*, 285–314.

Fettiplace, R. (2006). Active hair bundle movements in auditory hair cells. J. Physiol. (London) *576*, 29–36.

Frank, G., Hemmert, W., and Gummer, A.W. (1999). Limiting dynamics of high-frequency electromechanical transduction of outer hair cells. Proc. Natl. Acad. Sci. USA *96*, 4420–4425.

Gao, J., Wang, X., Wu, X., Aguiñaga, S., Huynh, K., Matsuda, K., Jia, S., Patel, M., Zheng, J., Cheatham, M.A., et al. (2007). Prestin-based outer hair cell electromotility in knockin mice does not appear to adjust the operating point of a cilia-based amplifier. Proc. Natl. Acad. Sci. USA *104*, 12542–12547.

Gold, T. (1948). Hearing II: the physical basis of the action of the cochlea. Proc. R. Soc. Lond. B. Biol. Sci. *135*, 492–498.

He, D.Z.Z., and Dallos, P. (1999). Somatic stiffness of cochlear outer hair cells is voltage dependent. Proc. Natl. Acad. Sci. USA *96*, 8223–8228.

He, D.Z.Z., Jia, S., and Dallos, P. (2004). Mechanoelectrical transduction of adult outer hair cells studied in the hemicochlea. Nature *429*, 766–770.

He, D.Z.Z., Zheng, J., Kalinec, F., Kakehata, S., and Santos-Sacchi, J. (2006). Tuning in the amazing outer hair cell: Membrane wizardry with a twist and shout. J. Membr. Biol. *209*, 119–134.

Howard, J., and Ashmore, J.F. (1986). Stiffness of sensory hair bundles in the sacculus ofthe frog. Hear. Res. *23*, 93–104.

Hudspeth, A.J. (1997). How hearing happens. Neuron *19*, 947–950.

Jia, S., and He, D.Z.Z. (2005). Motility-associated hair-bundle motion in mammalian outer hair cells. Nat. Neurosci. *8*, 1028–1034.

Jia, S., Dallos, P., and He, D.Z.Z. (2007). Mechanoelectric transduction of adult innner hair cells. J. Neurosci. *27*, 1006–1014.

Johnstone, J.R., Alder, V.A., and Johnstone, B.M. (1979). Cochlear action potential threshold and single unit thresholds. J. Acoust. Soc. Am. *65*, 254–257.

Keiler, S., and Richter, C.P. (2001). Cochlear dimensions obtained in hemicochlea of four different strains of mice: CBA/CaJ, 129/CD1, 129/SvEv and C57BL/6J. Hear. Res. *162*, 91–104.

Kennedy, H.J., Crawford, A.C., and Fettiplace, R. (2005). Force generation by mammalian hair bundles supports a role in cochlear amplification. Nature *433*, 880–883.

Kennedy, H., Evans, M.G., Crawford, A.C., and Fettiplace, R. (2006). Depolarization of cochlear outer hair cells evokes active hair bundle motion by two mechanisms. J. Neurosci. *26*, 2757–2766.

LeMasurier, M., and Gillespie, P.G. (2005). Hair cell mechanotransduction and cochlear amplification. Neuron *48*, 403–415.

Liberman, M.C., Gao, J.G., He, D.Z.Z., Wu, X.D., Jia, S.P., and Zuo, J. (2002). Prestin is required for electromotility of the outer hair cell and for the cochlear amplifier. Nature *419*, 300–304.

Manley, G.A. (2001). Evidence for an active process and a cochlear amplifier in nonmammals. J. Neurophysiol. *86*, 541–549.

Martin, P., and Hudspeth, A.J. (1999). Active hair bundle movements can amplify a hair cell's response to oscillatory mechanical stimuli. Proc. Natl. Acad. Sci. USA *96*, 14306–14311.

Narayan, S.S., Temchin, A.N., Recio, A., and Ruggero, M.A. (1998). Frequency tuning of basilar membrane and auditory nerve fibers in the same cochlea. Science *282*, 1882–1884.

Neely, S.T., and Kim, D.O. (1983). An active cochlear model showing sharp tuning and high sensitivity. Hear. Res. *9*, 123–130.

Patuzzi, R. (1996). Cochlear micromechanics and macromechanics. In The Cochlea, P. Dallos, A.N. Popper, and R.R. Fay, eds. (New York: Springer), pp. 186–257.

Ricci, A. (2003). Active hair bundle movements and the cochlear amplifier. J. Am. Acad. Audiol. *14*, 325–338.

Ricci, A.J., Kennedy, H.J., Crawford, A.C., and Fettiplace, R. (2005). The transduction channel filter in auditory hair cells. J. Neurosci. *25*, 7831–7839.

Robles, L., and Ruggero, M.A. (2001). Mechanics of the mammalian cochlea. Physiol. Rev. *81*, 1305–1352.

Russell, I.J., and Sellick, P.M. (1983). Low-frequency characteristics of intracellularly recorded receptor potentials in guinea-pig cochlear hair cells. J. Physiol. *338*, 179–206.

Ryan, A.F., and Dallos, P. (1975). Absence of cochlear outer hair cells: Effect on behavioural auditory threshold. Nature *253*, 44–46.

Rybalchenko, V., and Santos-Sacchi, J. (2003). Cl-flux through a non-selective, stretch-sensitive conductance influences the outer hair cell motor of the guinea pig. J. Physiol. *547*, 873–891.

Santos-Sacchi, J. (1991). Reversible inhibition of voltage-dependent outer hair cell motility and capacitance. J. Neurosci. *11*, 3096–3110.

Santos-Sacchi, J., Song, L., Zheng, J.F., and Nuttall, A.L. (2006). Control of mammalian cochlear amplification by chloride ions. J. Neurosci. *26*, 3992–3998.

Tsutakawa, R.K., and Hewett, J.E. (1978). Comparison of 2 regression lines over a finite interval. Biometrics *34*, 391–398.

Wu, X.D., Gao, J.G., Guo, Y.K., and Zuo, J. (2004). Hearing threshold elevation precedes hair-cell loss in prestin knockout m ice. Brain Res. Mol. Brain Res. *126*, 30–37.

Zheng, J., Shen, W., He, D.Z.Z., Long, K., Madison, L.D., and Dallos, P. (2000). Prestin is the motor protein of cochlear outer hair cells. Nature *405*, 149–155.

Zheng, J., Du, G.G., Matsuda, K., Orem, A., Aguiñaga, S., Deák, L., Navarrete, E., Madison, L.D., and Dallos, P. (2005). The C-terminus of prestin influences nonlinear capacitance and plasma membrane targeting. J. Cell Sci. *118*, 2987–2996.

Zheng, J., Du, G.G., Anderson, C.T., Keller, J.P., Orem, A., Dallos, P., and Cheatham, M.A. (2006). Analysis of the oligomeric structure of the motor protein prestin. J. Biol. Chem. *281*, 19916–19924.